A&A 490, 287–295 (2008)
DOI: 10.1051/0004-6361:200810379

Astronomy & Astrophysics

First time-series optical photometry from Antarctica

sIRAIT monitoring of the RS CVn binary V841 Centauri and the δ-Scuti star V1034 Centauri

K. G. Strassmeier[1], R. Briguglio[2,3], T. Granzer[1], G. Tosti[2], I. DiVarano[1], I. Savanov[1], M. Bagaglia[2], S. Castellini[2], A. Mancini[2], G. Nucciarelli[2], O. Straniero[4], E. Distefano[5], S. Messina[5], and G. Cutispoto[5]

[1] Astrophysical Institute Potsdam (AIP), An der Sternwarte 16, 14482 Potsdam, Germany
e-mail: [kstrassmeier;tgranzer;idivarano]@aip.de; isavanov@rambler.ru
[2] Dipartimento di Fisica, Università di Perugia, via A. Pascoli, 06100 Perugia, Italy
e-mail: [runa;gino.tosti]@fisica.unipg.it
[3] Concordia, Dome C, Antarctica; http://www.concordiabase.eu
[4] INAF – Osservatorio Teramo, via Mentore Maggini, 64100 Teramo, Italy
[5] INAF – Catania Astrophysical Observatory, via S. Sofia 78, 95123 Catania, Italy
e-mail: [sme;gcutispoto;edistefano]@oact.inaf.it

Received 12 June 2008 / Accepted 9 July 2008

ABSTRACT

Context. Eradicating the problems associated with the Earth's day-night cycle is mandatory for long and continuous time-series photometry and had been achieved with either large ground-based networks of observatories at different geographic longitudes or when conducted from space. A third possibility is offered by a polar location with astronomically-qualified site characteristics.
Aims. We present the first scientific stellar time-series optical photometry from Dome C in Antarctica and analyze approximately 13 000 CCD frames acquired in July 2007.
Methods. The optical pilot telescope of the "International Robotic Antarctic Infrared Telescope", named "small IRAIT" (sIRAIT), and its *UBVRI* CCD photometer were used in *BVR* for a continuous 243 h (10.15 days) with a duty cycle of 98% and a cadence of 155 s. The prime targets were the chromospherically active, spotted binary star V841 Cen and the non-radially pulsating δ-Scuti star V1034 Cen.
Results. We confirmed the known 0.2-day fundamental period of V1034 Cen and detected a total of 23 further periods between 2.2 h and 3.5 days. In July 2007, V841 Cen's V amplitude due to spots appeared to be at a record high of $0\overset{\mathrm{m}}{.}4$ in V. We completed a spot-model analysis with a light-curve inversion technique and discovered the star with a spot filling factor of 44% of the visible hemisphere, among the highest ever measured values for active stars, and a temperature-difference photosphere minus spot of 750 ± 100 K. Its odd-numbered (for a single site) rotation period was determined with a higher precision than before (5.8854 ± 0.0026 days), despite our comparably short data set. The rms scatter from a 2.4-h data subset was 3 mmag in V and 4.2 mmag in R. The differential data quality is 3–4 times higher than with the 25 cm Fairborn Automatic Photoelectric Telescope in southern Arizona and is probably due to the exceptionally low scintillation noise at Dome C.
Conclusions. We conclude that high-precision CCD photometry with exceptional time coverage and cadence can be acquired at Dome C in Antarctica and be successfully used to complete time-series astrophysics.

Key words. stars: starspots – stars: variables: general – stars: activity – stars: oscillations – stars: individual: V841 Centauri – stars: individual: V1034 Centauri

1. Introduction

Time-series photometry is a powerful tool for understanding cosmic variabilities and their many underlying physical mechanisms, from Gamma Ray Bursts to the non-radial oscillations of our Sun. World-wide networks around the globe have been established to reduce the disadvantages caused by the Earth's day-night cycle, e.g. by the "Global Oscillation Network Group" (Harvey et al. 1996), the "Whole Earth Telescope" (Nather et al. 1990), or the "Multi Site Continuous Spectroscopy" campaigns (Catala et al. 1993). Despite their tremendous success, these networks must cope with the many different site characteristics, the individual weather patterns, and, most importantly, with the different instrument/detector combinations and respective calibration issues. An alternative to these networks is a single polar site (e.g. Mosser & Aristidi 2007).

The French-Italian Antarctic station *Concordia* at Dome C at a height of 3200 m on the east Antarctic plateau is, besides the US South Pole station, the only plateau station populated over winter (=night). In principle, it enables astronomical observations comparable to regular observatories at temperate sites. Dome C received world-wide attention from the night-time astronomical community when the seeing conditions on the east Antarctic plateau were announced to be probably the highest quality on the entire planet with a median seeing of 0.3″ and occasionally even below 0.1″ at a height of approximately 30 m above the ground (Lawrence et al. 2004; Agabi et al. 2006).

Science cases that require continuous high-precision photometry uniquely benefit from the continuous 24-h day-night cycle and stable atmosphere. For example, δ Scuti stars are known to have a complex surface oscillation spectrum involving many modes and frequencies. The detection of patterns of

closely-spaced peaks in different modes enables the determination of the internal stellar structure. The essential observational restriction is the frequency resolution, which is proportional to the length of the photometric time series. It restricts the mode identification and their unique interpretation. Another example are spotted stars. Magnetic spots, such as those on the Sun, are tracers of the internal dynamo activity. Spot size and temperature are related to the magnetic flux that the emerging flux tube has transported from the solar interior. However, surface velocity fields such as differential rotation affect the magnetic field (and vice versa) so that spots are probably only indirectly linked with the dynamo. Observing the migration behavior of starspots from one stellar rotation to another, however, may constrain some global properties of the dynamo.

Optical photometry of bright stars can be completed at the photon-noise level because atmospheric scintillation noise appears to be a factor 3.6 smaller (Kenyon et al. 2006) than at the highest-quality temperate sites. The detailed issues for optical photometry from Dome C were highlighted by several authors, e.g. Vernin et al. (2007), Strassmeier (2007), and Kenyon et al. (2006). We note the experience gained from early attempts of the South Pole's "Vulcan-South" experiment[1] that, unfortunately, suffered from the particularly harsh winds at the South Pole.

A continuous 1500-h night opens a new window for science cases such as the search for extra-solar planets (e.g. Pont & Bouchy 2005; Deeg et al. 2005), asteroseismology (e.g. Fossat 2005; Mosser & Aristidi 2007), and stellar rotation and activity studies (e.g. Strassmeier & Oláh 2004). Several astronomical experiments are planned for Dome C (for a compilation see Strassmeier et al. 2007a). Among the pilot experiments is a small 25-cm optical precursor telescope for the 80-cm infrared telescope IRAIT (Tosti et al. 2006) and the 2 × 60 cm Schmidt-telescope ICE-T (Strassmeier et al. 2007b). sIRAIT was designed to experience the difficulties foreseen for the larger projects with the goal of completing full tests on a smaller scale.

We present and analyze the first data from sIRAIT from one CCD field obtained in July during winter 2007. Our primary target, V841 Cen, is a spotted, very active RS CVn binary with occasional flares and an orbital period so close to a multiple of a day (5.998 days) that time-series data from a single, non-polar site severely undersamples its light curve. Our secondary target is the δ-Scuti star V1034 Cen, a non-radially pulsating star in the lower part of the instability strip with a (likely) fundamental period of ≈0.2 days.

2. Instrumental set up and observations

2.1. sIRAIT

sIRAIT is a 25-cm, effective f/12 Cassegrain optical telescope on a parallactic mount located close to the *Concordia* station in the open field without a protection building (75°06′04″S, 123°20′52″E, 3233 m WGS84). Its CCD photometer is located approximately 1 m above the ground. The telescope was designed by the IRAIT team at the University of Perugia, Italy (Tosti et al. 2006) and built by the *Marcon* telescope factory of San Donà di Piave, Italy, equipped with electronics and installed at Dome C by one of the coauthors (Briguglio). It is equipped with a guiding refractor placed along the optical tube and moved by two extreme-environment stepper motors, originally designed for vacuum and suitable for very low temperatures.

[1] http://www.polartransits.org

The focal-plane unit contains the CCD camera, the filter wheel, two heaters, two fans, thermo-couples and Pt100 probes, the mirror adjustment device and other electronics. It is insulated by a thin layer of foam and is internally heated by two resistance heaters. The temperature achieved is constant to within 0.3 °C in the inner CCD box, and 5° ± 2 °C in the motor-drivers box. During acquisition, the CCD temperature is set at −28 °C. The photometer is a commercial MaxCam CCD camera by Finger Lakes Instruments (FLI). It is equipped with panchromatic Johnson *UBVRI* filters and a focusing device. A Kodak KAF-0402ME CCD with 768 × 512 9 μm pixels provides a field-of-view (FOV) of 8′ × 5.3′ with an image scale of 0.65″/pixel. Its quantum efficiency is given by the manufacturer to be 55% in *B*, 80% in *V*, and 60% in *R*. The full-well capacity is reached at 100 000 electrons and the FLI controller allows a read-out-noise of 15 electrons at nominal read-out speed of ≈500 kbit/s for a gain of 10 μV/e$^-$. From the flat-fields, we estimate a gain of 2.1 e$^-$/ADU and a read-out noise of 12.8 e$^-$, according to the procedure summarized by Janesick (1997). The typical point-spread-function (PSF) measured from a *V*-band frame is a Gaussian with a full-width at half maximum of 7.1 pixels (4.6″) for a star with $V = 9\overset{\text{m}}{.}0$, 30-s exposure, 16 000 ADU at peak, and a signal-to-noise ratio S/N = 12:1. This over-sampling of the PSF minimizes many practical problems such as the contribution of partial pixels at the PSF edge, variations in PSF due to e.g. focus changes, tracking and guiding errors, wind shake, or differential refraction, but at the expense of increased crowding by background stars.

2.2. Acquisition and reduction of photometric data

Both primary targets were in the same FOV of the CCD, which was centered at $\alpha = 14^{\text{h}}34^{\text{m}}40^{\text{s}}$ and $\delta = -60°25'$ (2000.0) (Fig. 1). The telescope acquired and tracked this FOV semi-automatically for a total of 243 continuous and consecutive hours (10.15 days) with only a single 5.8-h interruption (Fig. 2). Observations started at HJD 2 454 288.199. A total of 13 000 CCD frames were acquired. We note that the data were acquired during July 6–16, 2007, but the raw data arrived in Europe only at the end of January 2008 when the winter-over crew was able to leave the station.

A sequence of observations consisted of consecutive *BVR* frames with 60 s, 50 s, and 40 s integration times, respectively, typically allowing for approximately 20 images per hour per filter with an average time resolution of 155 s. Every day, approximately 20–30 min were requiring for telescope derotation to unwind the electric cabling, although this is barely noticeable in Fig. 2. A single 5.8-h gap occurred on the second day when the field was lost due to a tracking error. The counts per pixel were on average half of the full-well capacity of the CCD. The ratio of the sum of all background corrected pixels within the aperture (approximately 20 000 pixels) to the standard deviation of the background provides a peak S/N in *V* and *R* of 15 000 for V841 Cen ($V = 8\overset{\text{m}}{.}5$). We did not correct for cosmic-ray hits because these events were seldom and did not affect the photometry.

During the 10 days of acquisition, the weather was stable and good, with almost no wind, and temperatures of around −72° ± 2 °C. Ground-layer seeing varied between 2.8″ and an exceptional 5–6″. The few data acquired during the later stages of the observing period had internal deviations higher than 25 mmag and were rejected from the analysis (a total of ≈20 frames out of 13 000). A simple linear fit to a 2.4-h long *V* and *R* data subset measured a standard deviation of 3.0 and 4.2 mmag,

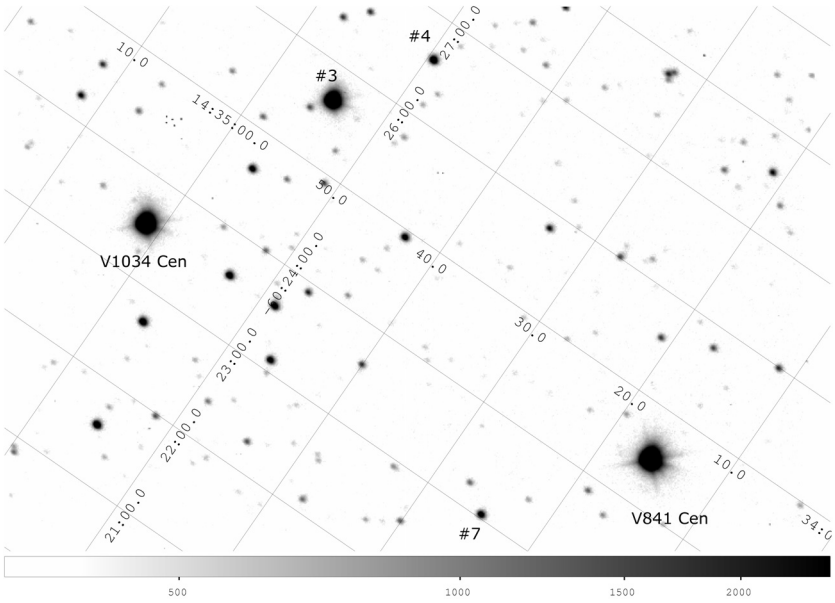

Fig. 1. Identification of stars in the CCD FOV (8′ × 5.3′). The three bright stars are our primary targets V841 Cen (*right*, $V = 8\overset{\mathrm{m}}{.}5$) and V1034 Cen (*left*) and the comparison star CD-59°5309 (*top*). The comparison star and stars #4 and #7 were identified as variable (see Table 1). The image shown is a composite of 20 individual *R*-band frames, each a 40-s integration. The coordinates are for equinox 2000.0. The faintest stars are of 16th magnitude.

respectively. We consider these as upper limits because the selected data-subset may not be free of intrinsic variability (see insert of Fig. 2).

Calibration frames were obtained three days after the science observations and consisted of 20 twilight flat fields in *BVRI* and a series of biases. Flat fields were acquired from horizon pointing during "midday" when the Sun was below the horizon but provided sufficient light for these exposures. Exposures of 30 s, 20 s, and 10 s for *B*, *V*, and *R*, respectively, and contained on average 20 000 counts. A data-cube fit to all 20 flat-field frames was performed to obtain a master flat. Dark frames were taken occasionally during the cable-derotation times to provide a total of 18, 25, and 26 frames for *B*, *V*, and *R*, respectively.

Twenty-five standard stars from Landolt (2007, and references therein) were observed ten times each on a clear night on September 10th, 2007 at the end of the Antarctic night. The air mass range was between 2−3 and unfortunately higher than for our science field observations. Large air-mass variations are impossible to observe at Dome C because of its high geographic latitude. Images were acquired in *UBVRI* but the *U* data had very poor S/N and were discarded. Even the *B* data had comparably large scatter in its photometric measurements. Extinction coefficients of $0\overset{\mathrm{m}}{.}278$, $0\overset{\mathrm{m}}{.}179$, $0\overset{\mathrm{m}}{.}064$, and $0\overset{\mathrm{m}}{.}081$ for *B*, *V*, *R* and *I*, respectively, were obtained from linear fits to the instrumental magnitudes versus air mass and then used to transform to the standard Johnson system (Briguglio 2008).

The designated comparison star was CD-59°5309. *Simbad*[2] lists it as a B-star with $V = 9\overset{\mathrm{m}}{.}50$, $B - V = +0\overset{\mathrm{m}}{.}74$, and $U - B = -0\overset{\mathrm{m}}{.}27$, according to its highest quality *UBV* values from Schild et al. (1983). Our data indicate that it is a low-amplitude variable star with $V = 9\overset{\mathrm{m}}{.}57$, a 1σ scatter of $0\overset{\mathrm{m}}{.}028$, and $V - R = 0\overset{\mathrm{m}}{.}44$. To increase the S/N ratio of its observations, we summed both three and ten consecutive *V* frames and performed a period analysis on both of the summed images. However, the noise in the summed 10-frame light curve appeared comparable to that in the individual frames, which we attribute to jitter from tracking errors which sometimes even includes jumps. Nevertheless, both data sets revealed periods of 3.04 days and 1.54 days as the most probable periods (both in a Scargle and a CLEAN application; see Sect. 4.1) but with low amplitudes comparable to the scatter in the data. Two additional periods of 5.57 and 0.983 days appear significant but have even lower amplitudes, while 6 additional periods are possible but are assessed to be unreliable due to the large amplitude of the noise. The residuals from a least-squares fit for all four periods is 0.05 mag. We conclude that the star is probably a non-radially pulsating B star with a fundamental period of either 3.0 or 1.5 days.

The CCD FOV contains an additional 60 stars that we were able to identify in NOMAD (Zacharias et al. 2005) with *V* magnitudes between $12\overset{\mathrm{m}}{.}4-15\overset{\mathrm{m}}{.}7$. None of these are, however, identified in *Simbad*. Two stars are possibly variable objects due to their higher-than-expected standard deviation and are listed in Table 1. No clear periods were found for either.

We employed the ARCO software package for CCD data reduction and analysis as described by Distefano et al. (2007). Standard CCD frame reduction consisted of bias and dark subtraction and flat-field division. We used the SExtractor (Bertin & Arnouts 1996) software to match stars detected in different CCD frames, selected the most appropriate candidates for an ensemble of comparison stars, and identified the parameters that optimized the photometry of each star and minimized the scatter in the light curves due to statistical fluctuations. Aperture photometry with an optimized aperture was then applied to all selected candidates of brightness between $R = 7\overset{\mathrm{m}}{.}9$ and $15\overset{\mathrm{m}}{.}7$. Figure 3 shows the scatter plot for *V* and *R* from a three-comparison star ensemble solution. We note that some stars were located so close to the edge of the FOV that they were sometimes unidentifiable by the photometry package, which resulted in artificially high residuals. These stars are not plotted in Fig. 3. An eye-ball fit to the lower envelope for ≈50 stars suggests a photometric precision of sIRAIT, for the range $12\overset{\mathrm{m}}{.}5$ to $15\overset{\mathrm{m}}{.}5$, of $0\overset{\mathrm{m}}{.}04$ at $12\overset{\mathrm{m}}{.}5$, and $0\overset{\mathrm{m}}{.}4$ at $15\overset{\mathrm{m}}{.}5$. For very bright targets, the precision is approximately 2.5 mmag above the expected scintillation-noise limit of 0.5 mmag (the full line in Fig. 3), while the faint stars are instrumental-noise limited (for a detailed discussion see Newberry 1991).

An estimate of the Dome-C sky brightness is obtained by using the background counts given by SExtractor for the dark-subtracted input frames (Fig. 4). We discarded all frames affected by twilight, i.e. during the fractional JD of between 0.5 and 0.85 as seen in Fig. 4. We note that moonlight did not contaminate our frames as we had waning moon. The maximum

[2] http://simbad.u-strasbg.fr/simbad/

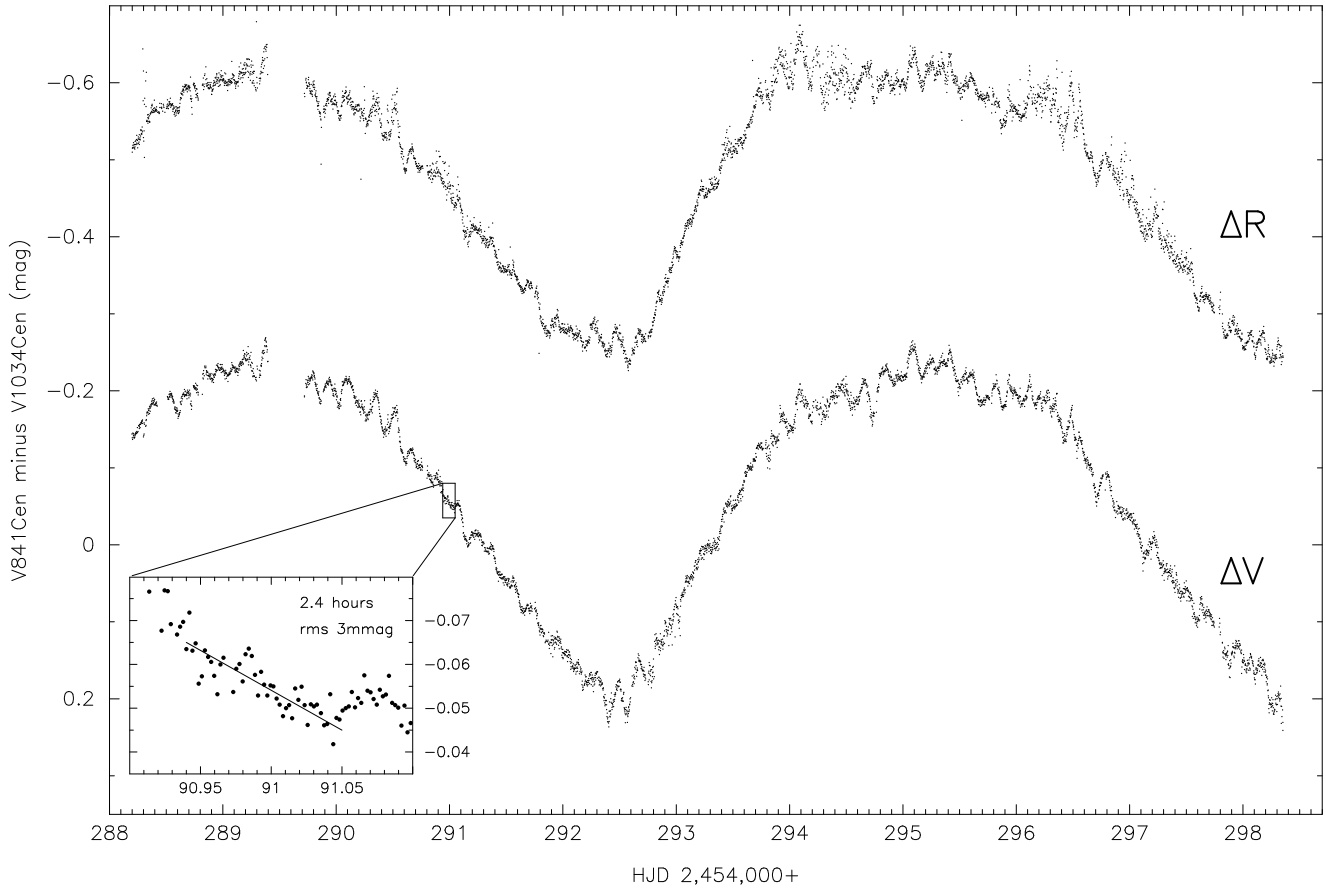

Fig. 2. Ten-day continuous differential *VR* photometry of V841 Cen minus V1034 Cen. Note that the long-period variation with an amplitude of $0\overset{m}{.}4$ in *V* is due to spots rotating in and out of view on V841 Cen, while the short-period variations with an amplitude of $\approx 0\overset{m}{.}02$ are due to non-radial pulsations of V1034 Cen. The insert shows a fraction of *V* data that is almost free of intrinsic short-term stellar variations. The residuals from a simple linear fit to a 2.4-h subset suggest a rms scatter of just 3 mmag in *V* (4.2 mmag in *R*). For this long duration, this is of 3–4 times higher quality than an equally sized telescope at a temperate site.

Table 1. Log of three other variable stars in the CCD FOV.

ID	NOMAD	α (in deg)	*V*	*R*	Notes
		δ (in deg)	σ_V	σ_R	
3	0295-0641140	218.72680	9.57	9.13	P = 3.0 d, 1.5 d
		–60.4277	0.028	0.028	
4	0295-0640999	218.70627	12.82	12.89	no clear P
		–60.4432	0.051	0.16	
7	0296-0615795	218.60366	13.14	13.17	no clear P
		–60.3841	0.24	0.25	

Note. ID is the internal identification according to Fig. 1. ID = 3 is the original comparison star CD-59°5309. NOMAD is the NOMAD catalog number (Zacharias et al. 2005). α and δ are for equinox 2000.0. *V* and *R* are their average magnitudes in the Johnson system, and σ_V and σ_R the standard deviations from the mean in the *V* and *R* bandpasses in magnitudes.

height of the moon above the horizon was 6° during the first night and 4° during the second night, after which it was continuously below the horizon, reaching new moon two days before the end of our campaign. The remaining frames showed average background count rates of 2.99, 4.65, and 6.83 ADU/pix in *B*, *V*, and *R*, respectively, at a rms of around 6.5 ADU. Converting these to sky brightnesses per square-arcseconds, we obtain magnitudes of $20\overset{m}{.}77$, $20\overset{m}{.}36$, $19\overset{m}{.}90$ in *B*, *V*, and *R*, respectively. We estimate that these values are good to within only $\approx 0\overset{m}{.}1$. Examples are shown in the inserts of Fig. 4. Our *V* value is possibly significantly brighter than the GATTINI-SBC estimate of $\approx$21 *V*mag/arcsec^2 converted from a Sloan *g* filter (Moore et al. 2007). Surprisingly, the background counts at midday varied by as high as a factor of four in *V* and *B*, and up to a factor of seven in *R*, which may have been caused by the illumination of high clouds. The ten-day rms at midnight was stable and converts into a sky-plus-detector limit of 1.88 mmag in *V*. This is indicated in Fig. 3 as a straight line.

2.3. Problems encountered

The spatially non-uniform gain of the CCD, which is dependent on both count-rate and time, did not allow the use of the original comparison star for high-precision differential photometry. This behavior was not noticed in pre-shipment CCD tests and is probably due to the controller or the environment in which it has been working in Antarctica. However, the *B* bandpass was irreparably affected by this due to its already low count rates and we did not use its data for further analysis.

Photometry for the full ensemble solution of 20 comparison stars had a scatter of more than twice the scatter for the two main targets than the differential magnitudes of the two bright stars themselves. The selection of the three next brightest and closest stars to V841 Cen as comparison stars resulted in a higher quality but more scattered light curve. We note that all these

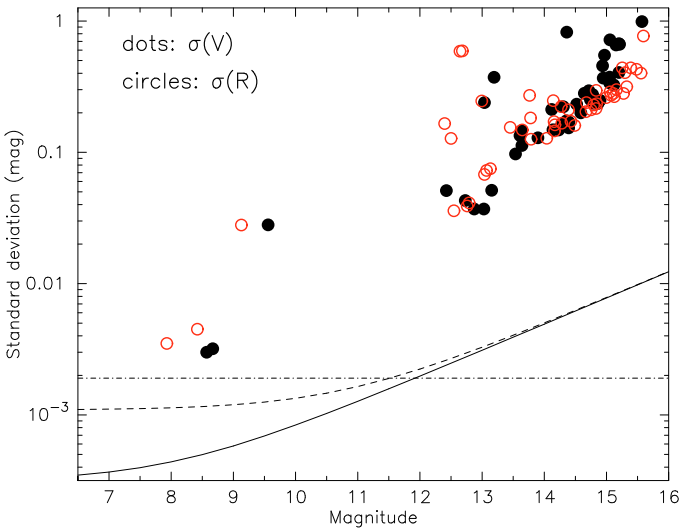

Fig. 3. *V* and *R*-band scatter diagram for an exposure time of 50 s (*V*) and 40 s (*R*). The precision for the two target stars ($V \approx 8\overset{m}{.}5$) was 3 mmag in *V* and 4.2 mmag in *R*. The lines indicate the sum of the photon and scintillation noise for a temperate site (dashed line) and for Dome C (full line). The horizontal dash-dotted line is an *estimate* of the convolved sky plus detector limit for sIRAIT.

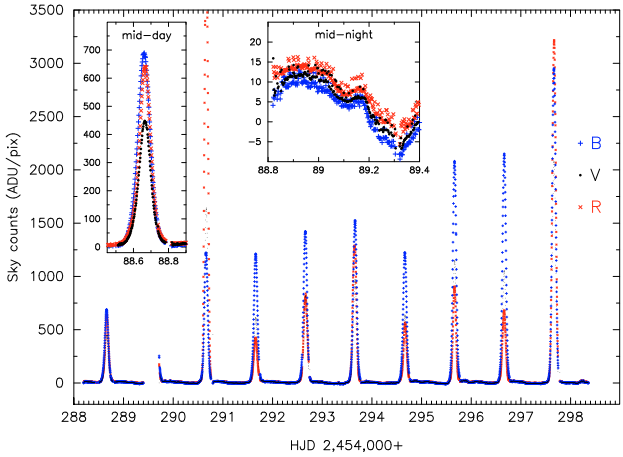

Fig. 4. Average background counts in *BVR* for the ten days of our observations. The inserts show an example of the counts during midday (*left*) and midnight (*right*), respectively. *BVR* is indicated with different plot symbols (pluses *B*, dots *V*, crosses *R*).

bona-fide comparison stars are at least four magnitudes fainter than our two target stars, and the differential magnitudes are accordingly noisier. We were able to overcome this problem and the gain problem, by using the δ-Scuti star V1034 Cen as the comparison star for V841 Cen (and vice versa) because it is the only star in the FOV with almost identical count rates.

Another problem occurred when the optics were cleaned twice during the night (at HJD 2 454 292.68 and 93.71). Although technically unrelated, this probably caused another CCD controller (or USB connection) problem due to unwanted interference. On both occasions, it suddenly decreased the count rate for V841 Cen, but increased the count rate for V1034 Cen (on the same exposure). Both count rates then exponentially re-settled to the previous (expected) count rates within ≈10 h. We have no explanation for this but we have attempted to model and remove the resettling trend with an exponential fit to the (differential) data. This introduced an extra scatter of ≈1 mmag during these 10 hours and the standard deviation became $\sqrt{3^2 + 1^2} \approx 3.2$ mmag.

We also noticed that the telescope had severe pointing and tracking errors that accumulated during the run. Repositioning was done manually after approximately an hour or so. A scatter plot of the central coordinates of all, for example *V* frames shows an elongated distribution with a peak-to-peak range of 100″ in both declination and right ascension. This implies that the FOV usable for continuous photometry is the minimum wrapped-in field from all individual pointings for a CCD FOV of 8′ × 5.3′. The range of 100″ is a significant restriction. This probably affected the photometric precision because the photometric aperture did not always enclose exactly the same pixels.

3. The primary target stars

3.1. V841 Cen = HD 127535

V841 Cen ($\alpha = 14^h34^m16^s$, $\delta = -60°24'27''$, 2000.0, $V = 8\overset{m}{.}5$) is a rapidly rotating, single-lined spectroscopic binary with an active K1 subgiant as its primary component (Collier 1982a). The star exhibits strong Ca II H&K and Hα emission (Houk & Cowley 1975; Weiler & Stencel 1979). It shows high X-ray flux in the ROSAT 0.1−2.4 keV energy range (Dempsey et al. 1993) and in the EUV (Mitrou et al. 1997), and also very high radio-flux densities (Slee & Stewart 1989). Its lithium abundance of $\log n = 0.77$ (Barrado y Navascués et al. 1998; but see also Randich et al. 1993, who obtained a significantly higher value) suggests a comparably young system. Randich et al. (1993) determined a $v \sin i$ of 33 ± 2 km s^{-1}, while De Medeiros et al. (1997) obtained 10 ± 1 km s^{-1} from CORAVEL tracings.

The orbit is circular with a period of 5.998 days (Collier 1982a), while the photometric (=rotational) period of the K1 subgiant was given by Cutispoto (1990) to be 5.929 ± 0.024 days. The orbital motion and the stellar rotation are therefore bound but not precisely synchronous, and/or the subgiant's surface is differentially rotating.

Previous photometry of V841 Cen was presented by Collier (1982b) from 1980−81, by Innis et al. (1998) from 1981, by Udalski & Geyer (1984) from 1984, by Bopp et al. (1986) from 1985, by Mekkaden & Geyer (1988) from April 1987, by Cutispoto (1990) from February 1987, by Cutispoto (1993) from 1989, by Cutispoto (1996) from Feb.−March 1990, by Cutispoto (1998a) from March 1991, by Cutispoto (1998b) from February 1992, by Strassmeier et al. (1994) from June−July 1994, and by Innis & Coates (2008). On one occasion, Cutispoto (1998a) detected a flare lasting at least one day. V841 Cen is listed under star number CABS 118 in the "Catalog of Chromospherically Active Binary Stars" (Strassmeier et al. 1993).

3.2. V1034 Cen = HD 127695

V1034 Cen ($\alpha = 14^h35^m01^s$, $\delta = -60°23'32''$, 2000.0, $V = 8\overset{m}{.}7$) is an A9IV δ-Sct star with a period of 0.235 days and a full amplitude of $0\overset{m}{.}03$ in *V* (Koen et al. 1999). Only one period is known, which is probably the fundamental period. A summary of known parameters was given by Rodriguez et al. (2000) in the revised δ-Sct catalog. The photometry by Koen et al. (1999) was obtained during 18 h on two consecutive nights and analyzed together. The authors mentioned that the *V*- and *B*-band phases were statistically identical but hinted that there may be additional low-amplitude frequencies. Koen et al. (1999) pointed out some target confusion in the Geneva photometry catalog

(Rufener 1988) that probably originated in observing V841 Cen instead of V1034 Cen.

4. Results and discussion

Figure 2 shows the entire time series of V841 Cen minus V1034 Cen for Johnson V and R. We note again that the comparison star CD-59°5309, which is one-magnitude fainter than the two target stars, could not be used because of a CCD-controller problem. Therefore, our first step was to separate the light variability of the two stars. Fortunately, this could be achieved reliably because the stars had significantly different variability periods and amplitudes.

4.1. The rotation period of V841 Cen

Our periodogram analysis for the combined V841 Cen minus V1034 Cen V data prominently shows the expected single frequency of around six days. We apply independently four different period-search routines to the combined differential data and then examine the pre-whitened output. Phase Dispersion Minimization (PDM, Lafler & Kinman 1965; Stellingwerf 1978) and Lomb-Scargle (LS, Scargle 1982) produce broad χ^2 minimums and, consequently, moderately well determined periods of 5.881 days and 5.884 days, respectively. The Minimum String Length (MSL, Dworetsky 1983) and the CLEAN algorithm (Roberts et al. 1987) provide a significantly sharper minimum and marginally longer periods of 5.8872 days and 5.8854 days, respectively. For consistency reasons, we adopt the CLEAN period to be the most likely rotation period of V841 Cen with an accuracy based on the rms of the four periods (0.0026 days). We note that an internal error of 10^{-6} days is obtained from the width of its χ^2 minimum by the criterium of Bevington (1969).

The surface rotation is synchronized to within 2% of the orbital period and appears to be of an older system, which conflicts with its relatively high lithium abundance. The K subgiant has an upper limit to its Li abundance that is about a factor of 10 below that considered to be a lithium-rich star but appears to have a higher than normal Li surface abundance (do Nascimento et al. 2003). High degrees of synchronization in the magnetically active component in RS CVn binaries is typical of the vast majority of systems with orbital periods of up to 30 days (Fekel & Eitter 1989).

4.2. The pulsation spectrum of V1034 Cen

The base rotational frequency of V841 Cen and up to 6 of its higher-order multiples are identified and subtracted from the combined light curve. The remaining V1034 Cen contribution is shown in Fig. 5a along with the least-squares fit from a total of 41 frequencies of which 24 are ranked significant according to the criterium of Breger (1993), which suggests a 99.9% probability for a peak not to be generated by noise if the obtained amplitude S/N exceeds 4.0. We note that the least-squares fit was obtained from the combined light curve, including the 7 frequencies needed to describe the V841 Cen light curve, but only the pre-whitened output is plotted in Fig. 5a. The final χ^2 achieved was 6.8 mmag, close to the average photometric precision. The periodogram for only the reconstructed V1034-Cen data is shown in Fig. 5b. Using the CLEAN approach, a total of 10 periods appear above a false-alarm probability (FAP) of 10^{-9} with peak-to-valley amplitudes in the range up to 12 mmag. Ten additional periods appear to have a FAP

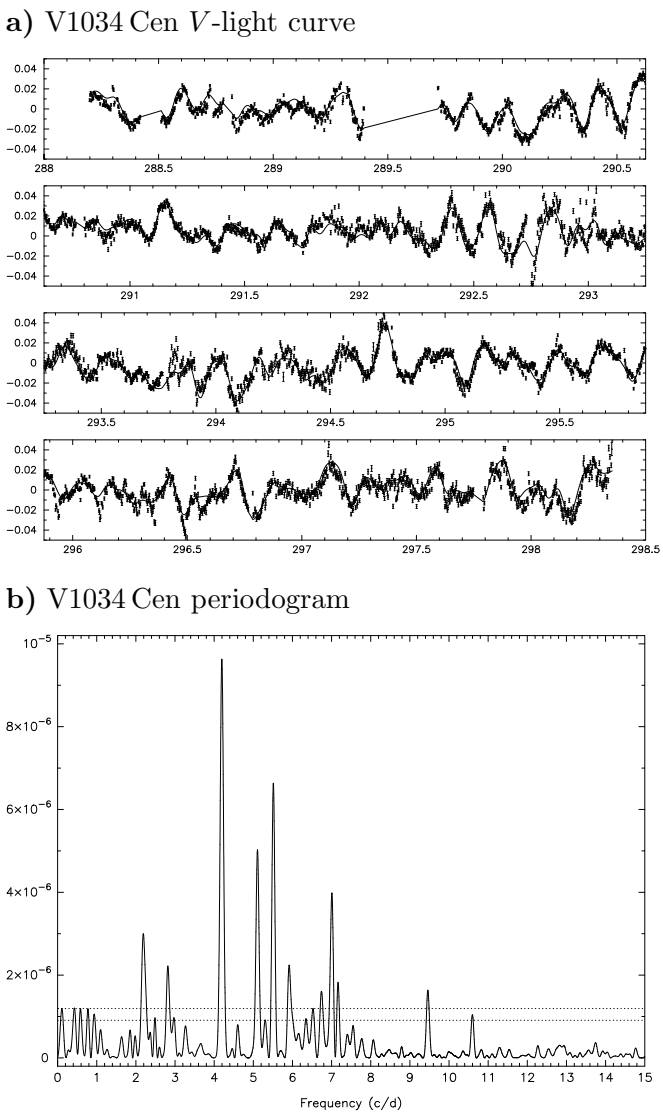

Fig. 5. a) V-light curve of V1034 Cen after reconstructing and subtracting the variation of V841 Cen. Time is in fractional Julian Date as in Fig. 2. Error bars are $\pm 1\sigma$. The line is the least-squares fit with the frequencies in Table 2. **b)** Period determination from a rectified CLEAN periodogram. The two horizontal lines indicate a false alarm probability of 10^{-6} (*lower line*) and 10^{-9} (*upper line*), respectively. A total of 20 periods between 2.2 h and 3.5 days appear above the 10^{-6} FAP. Note the complete absence of the one-day period and its aliases.

of above 10^{-6} with amplitudes below ≈6 mmag. Our frequency resolution from the full width at half maximum of the spectral window is 0.062 cycle/d. Frequencies lower than ≈0.2 cycle/d are problematic because these are close to the rotation cycle of the spotted star (0.17 cycle/d) and could be misinterpreted. For instance, a frequency of 0.145 cycle/d (Table 2) has an amplitude of 9.75 mmag and would be highly significant but is judged to be uncertain because its cycle length of 6.9 days is close to the duration of the entire data set and close to the rotation period of V841 Cen. In Table 2, we list all frequencies that we consider to be significant with respect to the data quality and the periodogram analysis. We note that the original frequency of ≈4.2 cycle/day (a period of ≈0.2 days) found by Koen et al. (1999) is recovered as the strongest peak in our data set in Fig. 5b at 4.20018 cycle/d, which confirms Koen et al.'s (1999) initial discovery.

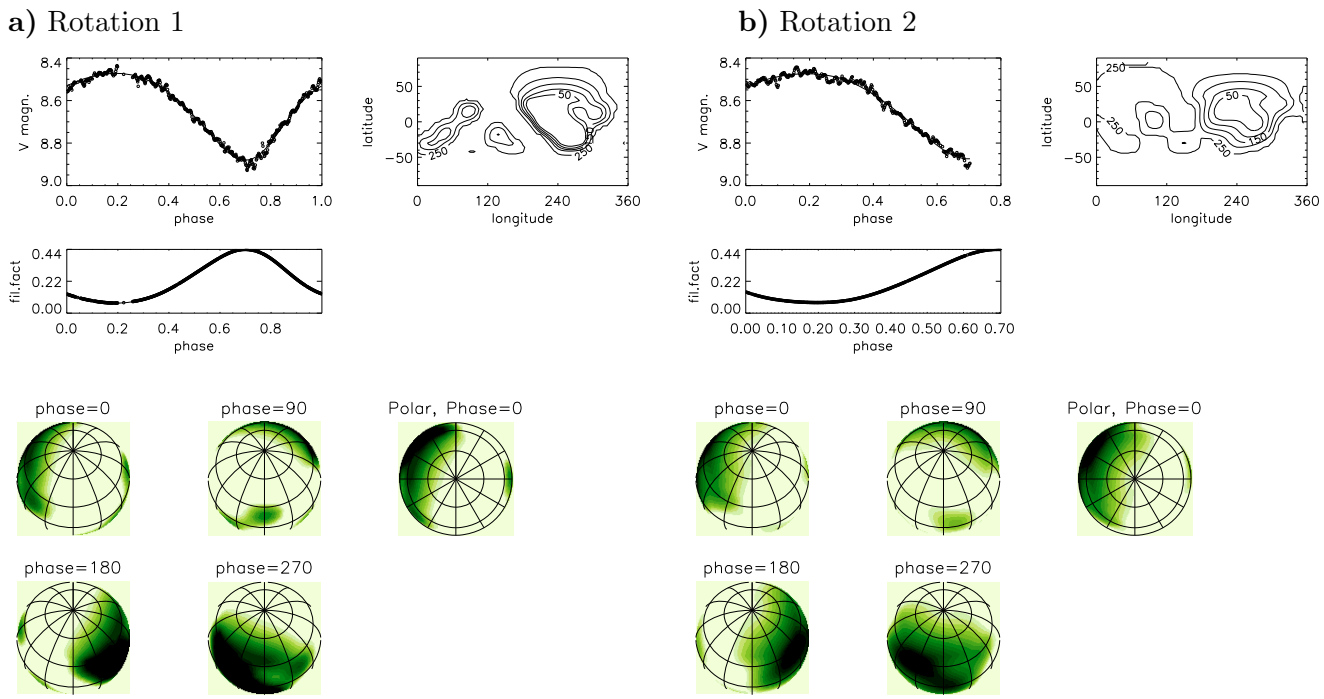

Fig. 6. A spot model for V841 Cen. **a)** Stellar rotation #1, **b)** stellar rotation #2. Each panel shows the fit to the V-band data (*top left*), the spot-filling factor in % per hemisphere as a function of rotational phase (*middle*), a contour spot map in Mercator projection (*top right*), and maps of the stellar surface in spherical and flattened pole-on view (entitled polar) in *the lower panels*. Note that phase zero coincides with our first data point.

4.3. A spot model for V841 Cen

We employ the new light-curve inversion code of Savanov & Strassmeier (2008). It reconstructs the stellar surface spot configuration from multi-color light curves by using a truncated least-squares estimation of the inverse problem's objects principal components. Our unknown object, the photospheric spot-filling factor, is a composite of a two temperature contribution; the intensity from the photosphere, I_P, and from cool spots, I_S, weighted by the fraction f of the surface covered with spots, i.e. the spot filling factor. The intensity per pixel is then

$$I = f \times I_P + (1 - f) \times I_S \quad (1)$$

with $0 < f < 1$. The inversion produces a distribution of spot filling factors over the visible stellar surface that reproduces the data most accurately. No assumptions about the shape, configuration, or total number of spots are made. The stellar astrophysical input includes band-pass fluxes calculated from atmospheric models from Kurucz (2000).

An effective temperature for V841 Cen of 4390 K was listed in Barrado y Navascués et al. (1998), who based their measurements on $V - I$ and $R - I$ indices. We note that the measurement of only $B - V$ would suggest a 300-K higher temperature of ≈4700 K based on e.g. Flower (1996). Karatas et al. (2004) measured a spectroscopic parallax that places V841 Cen at a distance of 63^{+26}_{-13} pc and with an accordingly uncertain luminosity of ≈2.3 $L_\odot$ (no *Hipparcos* parallax was available). Our most reliable rotation period of 5.8854 days and projected rotational velocity of 10 ± 1 km s^{-1} from De Medeiros et al. (1997) determine the lower limit of the stellar radius to be $R \sin i = 1.16 \pm 0.12\ R_\odot$. Assuming the luminosity based on the spectroscopic parallax and the Stefan-Boltzmann law, we obtain a matching radius only with inclinations of as low as 30° and 26° for effective temperatures of 4700 K and 4400 K, respectively. Cutispoto (1998b) favored a K3(V-IV) spectral type from the observed long-term *UBVRI* colors, which corresponds to a slightly higher inclination of ≈40° (±10°) and $T_{\rm eff}$ = 4500 K. These are the values that

Table 2. Period identifications for the δ Sct-star V1034 Cen.

No	Frequency (cycle/d)	Period (days)	Amplitude (mmag)	Notes
1	4.200	0.238	12.04	fundamental
2	5.514	0.181	9.91	stable
3	0.145	6.904	9.75	uncertain
4	0.461	2.169	9.71	uncertain
5	2.485	0.402	9.33	
6	5.107	0.196	8.90	stable
7	7.011	0.143	8.14	stable
8	0.766	1.304	7.80	uncertain
9	0.286	3.492	7.35	uncertain
10	2.192	0.456	6.87	
11	5.909	0.169	6.20	stable
12	6.738	0.148	5.94	stable
13	2.404	0.416	5.80	
14	7.161	0.140	5.78	stable
15	2.552	0.392	5.68	
16	9.462	0.106	5.09	stable
17	2.795	0.358	5.04	
18	2.941	0.340	5.02	
19	4.167	0.240	4.92	
20	6.509	0.154	4.41	
21	6.353	0.157	4.37	
22	10.600	0.094	4.11	stable
23	6.026	0.166	4.10	
24	5.294	0.189	4.04	

Note. The amplitude is the peak-to-valley V amplitude in milli-mag. Frequencies Nos. 11–24 are formally below the 1σ quality of the fit but are identified in the periodogram analysis in Fig. 5b. A "Stable" flag means that a frequency is mostly independent of other frequencies, "uncertain" means that the frequency is likely influenced by the length of the data set.

we adopt for the spot modeling. A generally low inclination is also in agreement with the low mass function of $f(m) = 0.025$ from the orbit by Collier (1982a) and the fact that we do see neither eclipses nor a secondary star in any of the published spectra (e.g. Randich et al. 1993). In any case, the numerical light-curve simulations by Savanov & Strassmeier (2008) demonstrated that a change in the inclination angle of even ±15° marginally altered the light-curve solution.

Due to the continuous time coverage, we do not need to convert the data into phase space but instead separate the data into first and second rotation based on a period of 5.8854 days. Five consecutive data points were always merged to an average value. Figure 6 shows the results for the consecutive 1.7 stellar rotations, dubbed "rotation 1" and "rotation 2". An enormous spot covering up to 44% of the visible hemisphere is required to reproduce the deep $0\overset{m}{.}4$ photometric minimum. A second, smaller spot with ≈10% filling factor at a longitude of ≈100° (phase $0\overset{p}{.}28$) located in the adjacent hemisphere is required to reproduce the broad shape of the light curve close to maximum light. We note that our inversion algorithm converges with a χ^2 of the fit that is always the (average) χ^2 of the data. Despite the low inclination of the rotational axis and the pronounced pole-on view, the inversion reconstructs both spots at low latitudes rather than at the poles. This is due to relatively sharp photometric minimum that precludes a polar, permanently-in-view location.

A spot coverage of 44% of the visible hemisphere is among the highest measured values for active stars and is, by chance, the same as that determined for the largest spot ever recorded by the Doppler-Imaging technique (for XX Tri, a K-giant in a 24-day RS CVn binary; Strassmeier 1999). However, spot sizes obtained from photometry depend on the spot temperature. The full $\Delta(V-R)$ amplitude in our data is $0\overset{m}{.}090 \pm 0.004$, becoming redder during minimum brightness and bluer during maximum brightness. Our inversion code reproduces this behavior with a most probable spot temperature of 3750 K. Its error is obtained from the numerical simulations in Savanov & Strassmeier (2008) that assume f increases by up to 30% if $\Delta T = T_P - T_S$ is lowered by 250 K. We conclude that $f = 44 \pm 3\%$ and $\Delta T = 750 \pm 100$ K are the most likely spot parameters for V841 Cen at the time of our observations.

Because the orbit determination is almost 30 years old and had a modestly precise period, it is impossible to identify the exact orbital phase at the time of our data in 2007. Therefore, no statement can be made regarding the location of the largest spot with respect to the orbital frame. However, this would be needed to interpret the magnetic-flux emergence in such a binary because the proximity of the companion star breaks the rotational symmetry and causes a non-uniform surface flux distribution (e.g. Holzwarth 2004).

5. Conclusions and outlook

We have presented 243 continuous hours of optical photometry from Antarctica with a duty cycle of 98% and a cadence of 155 s. A 3 mmag rms precision in V over 2.4 h with the 25-cm sIRAIT telescope was achieved for the two bright $8\overset{m}{.}5$ target stars. This is a factor of 3–4 higher than obtained with the 25-cm T1 automatic photoelectric telescope (APT) at Fairborn Observatory in southern Arizona (Strassmeier et al. 1997; Henry 1995). This is probably attributed to scintillation noise that is lower by a factor 3–4 than for temperate observing sites, as reported by Kenyon et al. (2006). We conclude that high-precision continuous photometry within the turbulent ground layer just one meter above ground is feasible at Dome C, even with low-cost, partly commercial components. The main problems that we encountered with sIRAIT in its first winterover were due to the quality of the equipment rather than with the harsh Antarctic environment. This makes us strongly believe that our proposed 2 × 60-cm, more optimized and robust, photometric facility ICE-T (Strassmeier et al. 2007b) and the intermediate-step 40 cm *a-step* experiment (Fressin et al. 2007) are well suited for a site such as Dome C and could, in some favorable cases, even challenge photometry from space.

Acknowledgements. The field activities and the results at Dome C benefit from the support of the French and Italian polar agencies IPEV and PNRA in the framework of the Concordia station programme. We tank the AstroConcordia astronomers D. Mékarnia and F. Jeanneaux for their support during the winterover. Heidi Korhonen kindly provided the scintillation noise values for temperate sites. We thank an anonymous referee for several helpful suggestions that improved the paper. German participation in sIRAIT was financed by AIP through the State of Brandenburg and the federal Ministry of Education and Research and supported by the German polar agency AWI. Discussions with Michel Breger on the significance of pulsation frequencies is also appreciated. Finally, we acknowledge support from the European Community's Sixth Framework Programme under contract number RICA-026150 (ARENA).

References

Agabi, A., Aristidi, E., Azouit, M., et al. 2006, PASP, 118, 344
Bertin, E., & Arnouts, S. 1996, A&AS, 117, 393
Bevington, P. R. 1969, Data Reduction and Error Analysis for the Physical Sciences (New York: McGraw-Hill)
Briguglio, R. 2008, Ph.D. Thesis, Univ. of Perugia
Barrado y Navascués, D., De Castro, E., Fernández-Figueroa, M., Cornide, M., & Garcia López, R. J. 1998, A&A, 337, 739
Bopp, B. W., Africano, J., & Quigley, R. 1986, AJ, 92, 1409
Breger, M., Stich, J., Garrido, R., et al. 1993, A&A, 271, 482
Catala, C., Foing, B. H., Baudrand, J., et al. 1993, A&A, 275, 245
Collier, A. C. 1982a, Ph.D. Thesis (New Zealand: University of Canterbury)
Collier, A. C. 1982b, Southern Stars, 30, 177
Cutispoto, G. 1990, A&AS, 84, 397
Cutispoto, G. 1993, A&AS, 102, 655
Cutispoto, G. 1996, A&AS, 119, 281
Cutispoto, G. 1998a, A&AS, 127, 207
Cutispoto, G. 1998b, A&AS, 131, 321
Dempsey, R. C., Linsky, J. E., Fleming, T., & Schmitt, J. H. M. M. 1993, ApJS, 86, 599
Deeg, H. J., Belmonte, J. A., Alonso, R., et al. 2005, in Dome C, ed. M. Giard et al., EAS Publ. Ser., 14, 303
De Medeiros, J. R., Do Nascimento, J. D., & Mayor, M. 1997, A&A, 317, 701
Distefano, E., Messina, S., Cutispoto, G., et al. 2007, in Large Astronomical Infrastructures at Concordia, Roscoff, ed. N. Epchtein et al., EAS Publ. Ser., 25, 165 (EDP sciences)
Do Nascimento, J. R., Canto Martins, B. L., Melo, C. H. F., Porto Mello, G., & De Medeiros, J. R. 2003, A&A, 405, 723
Dworetsky, M. M. 1983, MNRAS, 203, 917
ESA 1997, The Hipparcos and Tycho Catalogues, ESA SP-1200
Fekel, F. C., & Eitter, J. J. 1989, AJ, 97, 1139
Flower, P. J. 1996, ApJ, 469, 355
Fossat, E. 2005, in Dome C, Astronomy, and Astrophysics Meeting, ed. M. Giard et al., EDP Publ. Ser., 14, 121
Fressin, F., Guillot, T., Schmider, F.-X., et al. 2007, in Large Astronomical Infrastructures at Concordia, Roscoff, ed. N. Epchtein et al., EAS Publ. Ser., 25, 225 (EDP sciences)
Harvey, J. W., Hill, F., Hubbard, R., et al. 1996, Science, 272, 1284
Henry, G. W. 1995, in Robotic Telescopes: Current Capabilities, Present Developments, and Future Prospects for Automated Astronomy, ed. G. W. Henry, & J. A. Eaton, ASP Conf. Ser., 79, 37
Holzwarth, V. 2004, AN, 325, 408
Houk, N., & Cowley, A. 1975, Michigan Catalog, 1, Ann Arbor: Astron. Dept.
Innis, J. L., & Coates, D. W. 2008, IBVS, 5838
Innis, J. L., Thompson, K., & Coates, D. W. 1998, IBVS, 4570
Janesick, J. 1997, SPIE, 3019, 70
Karatas, Y., Bilir, S., Eker, Z., & Demircan, O. 2004, MNRAS, 349, 1069
Kenyon, S. L., Lawrence, J., Ashley, M. C. B., et al. 2006, PASP, 118, 924
Koen, C., Van Rooyen, R., Van Wyk, F., & Marang, F. 1999, MNRAS, 309, 1051
Kurucz, R. L. 2000, http://www.cfaku5.harvard.edu
Lafler, J., & Kinman, T. D. 1965, ApJS, 11, 216

Landolt, A. U. 2007, AJ, 133, 2502
Lawrence, J. S., Ashley, M. C. B., Tokovinin, A., & Travouillon, T. 2004, Nature, 431, 278
Mekkaden, M. V., & Geyer, E. H. 1988, A&A, 195, 214
Mitrou, C. K., Mathioudakis, M., Doyle, J. G., & Antonopoulov, E. 1997, A&A, 317, 776
Moore, A., Aristidi, E., Ashley, M., et al. 2007, in Large Astronomical Infrastructures at Concordia, Roscoff, EDP sciences, ed. N. Epchtein et al., EAS Publ. Ser., 25, 35
Mosser, B., & Aristidi, E. 2007, PASP, 119, 127
Nather, R. E., Winget, D. E., Clemens, J. C., Hansen, C. J., & Hine, B. P. 1990, ApJ, 361, 309
Newberry, M. V. 1991, PASP, 103, 122
Pont, F., & Bouchy, F. 2005, in Dome C, Astronomy, and Astrophysics Meeting, ed. M. Giard et al., EDP Publ. Ser., 14, 155
Randich, S., Gratton, R., & Pallavicini, R. 1993, A&A, 273, 194
Roberts, D. H., Lehár, J., & Dreher, J. W. 1987, AJ, 93, 968
Rodriguez, E., Lopez-Gonzalez, M. J., & Lopez de Coca, P. 2000, A&AS, 144, 469
Rufener, F. 1988, Catalogue of Stars measured in the Geneva Observatory Photometric System, 4th edn., Geneva Obs., Sauverny
Savanov, I. S., & Strassmeier, K. G. 2008, AN, 329, 364
Scargle, J. D. 1982, ApJ, 263, 835
Schild, R. E., Garrison, R. F., & Hiltner, W. A. 1983, ApJS, 51, 321
Slee, O. B., & Stewart, R. T. 1989, MNRAS, 236, 129
Stellingwerf, R. F. 1978, ApJ, 224, 953
Strassmeier, K. G. 1999, A&A, 347, 225
Strassmeier, K. G. 2007, in Large Astronomical Infrastructures at Concordia, Roscoff, EDP sciences, ed. N. Epchtein et al., EAS Publ. Ser., 25, 233
Strassmeier, K. G., & Oláh, K. 2004, ESA SP-583, 149
Strassmeier, K. G., Hall, D. S., Fekel, F. C., & Scheck, M. 1993, A&AS, 100, 173
Strassmeier, K. G., Paunzen, E., & North, P. 1994, IBVS, 4066
Strassmeier, K. G., Bartus, J., Cutispoto, G., & Rodonó, M. 1997, A&AS, 125, 11
Strassmeier, K. G., Agabi, K., Agnoletto, L., et al. 2007a, AN, 328, 451
Strassmeier, K. G., Andersen, M., Granzer, T., et al. 2007b, in Transiting Extrasolar Planets Workshop, ed. C. Afonso et al. (ASP), 366, 332
Tosti, G., Busso, M., Nucciarelli, G., et al. 2006, SPIE, 6267, 47
Udalski, A., & Geyer, E. H. 1984, IBVS, 2594
Vernin, J., Agabi, K., Aristidi, E., et al. 2007, in Large Astronomical Infrastructures at Concordia, Roscoff (EDP sciences), ed. N. Epchtein et al., EAS Publ. Ser., 25, 23
Walker, G. A. H., Croll, B., Kuschnig, R., et al. 2007, ApJ, 659, 1611
Weiler, E. J., & Stencel, R. E. 1979, AJ, 84, 1372
Zacharias, N., Monet, D. G., Levine, S. E., et al. 2005, BAAS, 36, 1418